Biochimica et Biophysica Acta 1788 (2009) 2462–2470

Contents lists available at ScienceDirect

Biochimica et Biophysica Acta

journal homepage: www.elsevier.com/locate/bbamem

Effects of PKA phosphorylation on the conformation of the Na,K-ATPase regulatory protein FXYD1

Peter Teriete, Khang Thai, Jungyuen Choi, Francesca M. Marassi *

Burnham Institute for Medical Research, 10901 North Torrey Pines Road, La Jolla, CA 92037, USA

ARTICLE INFO

Article history:
Received 8 July 2009
Received in revised form 21 August 2009
Accepted 6 September 2009
Available online 15 September 2009

Keywords:
FXYD
Phospholemman
Na,K-ATPase
Phosphorylation, Structure
NMR
Micelle

ABSTRACT

FXYD1 (phospholemman) is a member of an evolutionarily conserved family of membrane proteins that regulate the function of the Na,K-ATPase enzyme complex in specific tissues and specific physiological states. In heart and skeletal muscle sarcolemma, FXYD1 is also the principal substrate of hormone-regulated phosphorylation by c-AMP dependent protein kinase A and by protein kinase C, which phosphorylate the protein at conserved Ser residues in its cytoplasmic domain, altering its Na,K-ATPase regulatory activity. FXYD1 adopts an L-shaped α-helical structure with the transmembrane helix loosely connected to a cytoplasmic amphipathic helix that rests on the membrane surface. In this paper we describe NMR experiments showing that neither PKA phosphorylation at Ser68 nor the physiologically relevant phosphorylation mimicking mutation Ser68Asp induces major changes in the protein conformation. The results, viewed in light of a model of FXYD1 associated with the Na,K-ATPase α and β subunits, indicate that the effects of phosphorylation on the Na,K-ATPase regulatory activity of FXYD1 could be due primarily to changes in electrostatic potential near the membrane surface and near the Na^+/K^+ ion binding site of the Na,K-ATPase α subunit.

1. Introduction

The FXYD proteins constitute a family of regulatory subunits of the Na,K-ATPase ion pump, the principal enzyme responsible for maintaining the gradient of Na^+ and K^+ ion concentrations across cell membranes [1–3]. The enzyme complex is formed by a catalytic α subunit (110 kDa), an auxiliary β subunit (31–kDa), and a regulatory FXYD subunit (7–17 kDa). The known isoforms of the three subunits, α1-α4, β1-β3, and FXYD1-FXYD10, show a high level of subunit-specific sequence similarity and their expression is tissue-specific as well as developmentally regulated [4,5]. The energy required to exchange 3 Na^+ ions for 2 K^+ ions across the plasma membrane is generated by the hydrolysis of ATP in the cytosol, through a process involving distinct intermediate states of the enzyme that is regulated by the FXYD proteins.

The FXYD family proteins have been reported to induce distinct, and sometimes opposing, effects on the enzyme's rate constant and on its affinity for intracellular Na^+ or extracellular K^+ ions [1–3]. These differences have been ascribed to specific differences in the amino acid sequences of the FXYD transmembrane domains, which are otherwise highly conserved throughout the protein family, and to differences in the cytoplasmic domains, whose sequences vary widely among the FXYD family members. The FXYD structures mirror the intron–exon arrangements of their corresponding genes, suggesting that the polypeptides are assembled from discrete structured domains that may have evolved to confer different functional properties in various physiological settings [6]. The FXYD activities are also modulated by post-translational modifications, including phosphorylation (FXYD1) and glycosylation (FXYD5). For example, in heart and skeletal muscle, FXYD1 (PLM; phospholemman) is the principal substrate of hormone-stimulated phosphorylation by c-AMP dependent protein kinase A (PKA) and protein kinase C (PKC), which specifically phosphorylate the protein either at Ser68 (PKA), or at Ser63, Ser68 and Thr69 (PKC) in its cytoplasmic domain [7–9]. Functional studies in cells indicate that phosphorylation of FXYD1 can influence the protein activity in at least two ways: either indirectly, by regulating the level of FXYD1 expression at the plasma membrane, or directly, by altering the functional properties of FXYD1 associated with the Na,K-ATPase at the plasma membrane [9,10].

Phosphorylation of FXYD1 is a key factor regulating the delivery of FXYD1 from the endoplasmic reticulum (ER) to the plasma membrane [9]. The last three arginines at the C-terminus of FXYD1 resemble the RXR motif implicated in the ER retention of multimeric membrane proteins (reviewed in [11]). Notably, the ER-retention sequence of one such protein, the NR1 subunit of the NMDA receptor, is regulated by coordinated PKA/PKC phosphorylation at specific sites in its vicinity [12]; phosphorylation is thought to screen the positively charged ER-retention signal and, thus, enable the NR1 subunit to traffic from the ER. PKA phosphorylation of NR1 appears to be constitutive in all secretory compartments and to be required for efficient PKC

* Corresponding author. Tel.: +1 858 795 5282; fax: +1 858 713 6268.
E-mail address: fmarassi@burnham.org (F.M. Marassi).

0005-2736/$ – see front matter © 2009 Elsevier B.V. All rights reserved.
doi:10.1016/j.bbamem.2009.09.001

phosphorylation, however, once PKA/PKC-phosphorylated NR1 exits the ER it is rapidly dephosphorylated at PKC sites. Interestingly, the amount of FXYD1 expressed in oocyte membranes is increased by co-expression of PKA [13]. Furthermore, the pattern of PKA/PKC phosphorylation in the C-terminus of FXYD1 resembles that of the NMDA NR1 ER-retention sequence (Fig. 1), suggesting that a similar mechanism may operate to regulate FXYD1 export from the ER to the plasma membrane. Further underscoring the importance of the indirect effects of phosphorylation on pump activity, PKA/PKC phosphorylation of the Na,K-ATPase α subunit has also been shown to regulate trafficking of the pump from intracellular organelles to the plasma membrane, thereby affecting the pump expression level and activity [14].

FXYD1 phosphorylation has also been reported to relieve FXYD1 inhibition of the Na,K-ATPase through the direct functional interaction of FXYD1 with the pump [10,15–19]. Specifically, the co-expression of FXYD1 with α1/β1 or α2/β1 isozymes in oocytes or in HeLa cells causes a significant decrease in the affinity of the Na,K-ATPase for Na^+ ions, with a smaller decrease in their affinity for K^+ ions and little effect on the transport rate [20,21], and both α1, which is found in nearly all animal tissues, and α2, which is highly expressed in heart and skeletal muscle, are specifically stabilized by FXYD1 [22]. PKA phosphorylation of FXYD1 reverses these effects, increasing the apparent Na^+ affinity of both α1/β1 and α2/β1 isozymes, with no effect on their apparent K^+ affinity nor on their maximal transport activity, whereas PKC phosphorylation selectively increases the maximal pump current of the α2/β1 but not α1/β1 isozyme [10]. These effects of phosphorylated FXYD1 (pFXYD1) on Na,K-ATPase activity are recapitulated in a mutant form of FXYD1 where Ser63 and Ser68 were changed to Asp to mimic the effects of phosphorylation [10]. Finally, in cardiac myocytes isolated from FXYD1 knockout mice, the Na,K-ATPase activity was increased significantly [15,17,18,23], indicating that FXYD1 plays an important role in heart contractile function. In contrast, overexpression of FXYD1 in wild-type myocytes reduced Na,K-ATPase activity [24], while FXYD1 phosphorylation by PKA and PKC increased it [15–19].

The direct effects of FXYD1 phosphorylation on Na,K-ATPase activity have been proposed to reflect a major change in the conformation of FXYD1, however, no structural information has been available for the phosphorylated protein and the nature of the conformational change is not known. In this paper we report the effects of PKA phosphorylation on the three-dimensional structure of FXYD1 examined by NMR spectroscopy.

Two crystal structures of the Na,K-ATPase were recently reported, one determined at 3.5 Å resolution for the α1/β1/FXYD2 complex isolated from pig kidney [25], and the other determined at 2.4 Å resolution for the α3/β1/FXYD10 complex isolated from shark rectal glands [26]. In both structures, the pump is in the E2 occluded ion conformation and is in complex with occluded Rb^+ ions acting as substitutes for the K^+ ions that would be found *in vivo*. The structures identify the arrangement of the cytoplasmic domain and ten transmembrane helices of the α subunit, and show that the β subunit transmembrane helix associates with transmembrane helices αM7 and αM10, while the FXYD protein transmembrane helix associates with transmembrane helix αM9. However, no structural information could be obtained for the β and FXYD cytoplasmic domains due to lack of electron density.

Recently, we determined the NMR structure of non-phosphorylated FXYD1 in detergent micelles [27]. The N-terminal transmembrane domain forms three rigidly connected helices (h1, h2, h3) and shares both significant amino acid sequence homology [5] as well as structural similarity [6,28] with the other FXYD proteins (Fig. 1). It is loosely connected to a 10-residue C-terminal cytoplasmic helix (h4) with a sequence unique to FXYD1, which contains the phosphorylation domain. Helix h4 is flanked by an N-terminal acidic sequence (DEEE) and a C-terminal basic ER-retention sequence (RRR) that are important for mediating trafficking from the ER [9], and rests on the membrane surface exposing the phosphorylation sites (Ser63, Ser68 and Thr69) to the aqueous phase. This helix is highly basic, which helps explain its propensity to associate with a negatively charged micelle/membrane surface, however, it is connected to the rest of the protein by a relatively long flexible linker, indicating that it would be capable of adopting a different orientation in its interaction with the Na,K-ATPase α subunit and of undergoing reorientation upon phosphorylation.

We find that neither phosphorylation at Ser68 nor the Ser68Asp mutation mimicking PKA phosphorylation cause major changes in protein conformation, and that both appear to induce only a modest increase in the mobility of the cytoplasmic helix. Together with a model of FXYD1 bound to the Na,K-ATPase α subunit, the NMR results indicate that the effects of phosphorylation on the Na,K-ATPase regulatory activity of FXYD1 could be due primarily to the localization and movement of charged residues at the membrane surface and, possibly, near the Na^+/K^+ ion binding sites of the pump.

2. Materials and methods

2.1. Sample preparation

Uniformly ^{15}N-labeled FXYD1 and FXYD1(S68D) were expressed, purified, and characterized as described previously [29]. The Ser68Asp mutation was generated using the QuickChange mutagenesis kit (Stratagene) and verified by DNA sequencing. Purified FXYD1 was phosphorylated with PKA by dissolving 1 mg of protein in 2 mL of buffer A (50 mM HEPES, pH 5; 25 mM $MgCl_2$, 25 mM NaF, 1 mM EGTA, 0.1% triton X-100, 1 mM ATP), adding 20 μg of PKA, and gently mixing for 5 h at 30 °C. To stop the reaction, PKA was inactivated by adding SDS to a final concentration of 4 mM. pFXYD1 was isolated from the

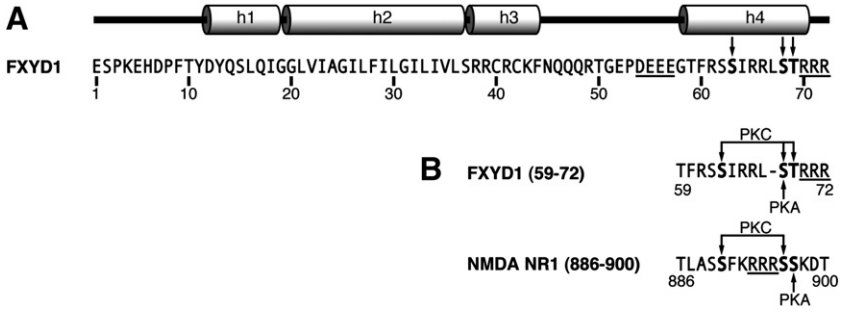

Fig. 1. Amino acid sequence and secondary structure of human FXYD1 (NCBI: NP_068702) and comparison with human NMDA receptor NR1 subunit (NCBI: NP_015566). (A) Mature full length FXYD1. The S63, S68, T69 phosphorylation sites are marked with arrows. Acidic (DEEE) and basic (RRR) sequences important for ER export are underlined. (B) Phosphorylation domains of FXYD1 and NMDA NR1. Arrows mark the PKA and PKC phosphorylation sites. The ER-retention signals (RRR) are underlined.

reaction mixture by size exclusion chromatography (Sephacryl S-300, Amersham) in buffer B (10 mM sodium phosphate, pH 7.5, 12 mM DTT, 4 mM SDS). The fractions containing pFXYD1 were pooled and concentrated to 1 mL in a stirred cell (Amicon) with a dialysis membrane of 5 kDa molecular weight cutoff. After a brief (5 h) dialysis against water, the resulting solution was lyophilized and stored at −20 °C.

Previous analysis with an antibody specific for Ser68-phosphorylated FXYD1 demonstrated that this procedure phosphorylates FXYD1 specifically at Ser68 [30]. Phosphorylation was ascertained by SDS-PAGE, by MALDI-TOF mass spectrometry performed as described previously [29], by performing a pilot reaction with ^{32}P-labeled ATP, and by ^{31}P NMR spectroscopy (Fig. 2). SDS-PAGE was performed with the Tris-Tricine system [31].

Solution NMR samples were prepared by dissolving pure lyophilized protein in 300 μL of NMR buffer (20 mM sodium citrate pH 5, 10 mM DTT, 10% D_2O, and 500 mM SDS). High purity (>98%) SDS (obtained from Calbiochem or Cambridge Isotopes Laboratories) was used for protein purification and for the NMR samples.

2.2. NMR experiments and data analysis

The ^{1}H/^{15}N NMR correlation spectra were obtained with the standard fast HSQC (heteronuclear single quantum coherence) experiment [32]. Backbone resonances of pFXYD1 and FXYD1(S68D) were assigned using the three-dimensional ^{15}N-NOESY-HSQC experiment [33] with a NOESY mixing time of 150 ms, and by comparison with the spectrum of FXYD1 which had been previously assigned [6,27]. For the $MnCl_2$ paramagnetic broadening experiments, the resonance intensities in the ^{1}H/^{15}N HSQC spectrum of FXYD1(S68D) were measured with a sample containing 1.8 mM $MnCl_2$. All NMR experiments were performed at 40 °C on a Bruker AVANCE 600 MHz spectrometer. Chemical shifts were referenced to the H_2O resonance set to its expected position at 40 °C [34]. ^{31}P NMR spectra were referenced with phosphoric acid. The NMR data were processed using NMRPipe [35], and the spectra were assigned and analyzed using Sparky [36].

Dihedral angles were derived from analysis of the NMR chemical shifts with the program TALOS [37]. The program uses chemical shifts and amino acid sequence information to search a database of protein structures and chemical shifts, and predicts the protein backbone dihedral angles ϕ and ψ. For α-helices, TALOS predictions are typically classified as "good" if all of the 10 best database matches occur in the phi < 0 half of the Ramachandran plot, and at least 9 of the 10 best matches are in a consistent (within a 35° standard deviation) ϕ/ψ region. However, if the 10 best matches have mutually inconsistent values of ϕ and ψ, the results are classified as ambiguous, and no dihedral angle prediction is made. Fig. 5B shows "good" TALOS predictions obtained for FXYD1 and pFXYD1 using only N and HA chemical shifts, and compares the results to those obtained for FXYD1 using the previously measured N, HA, CA and CB chemical shifts [27].

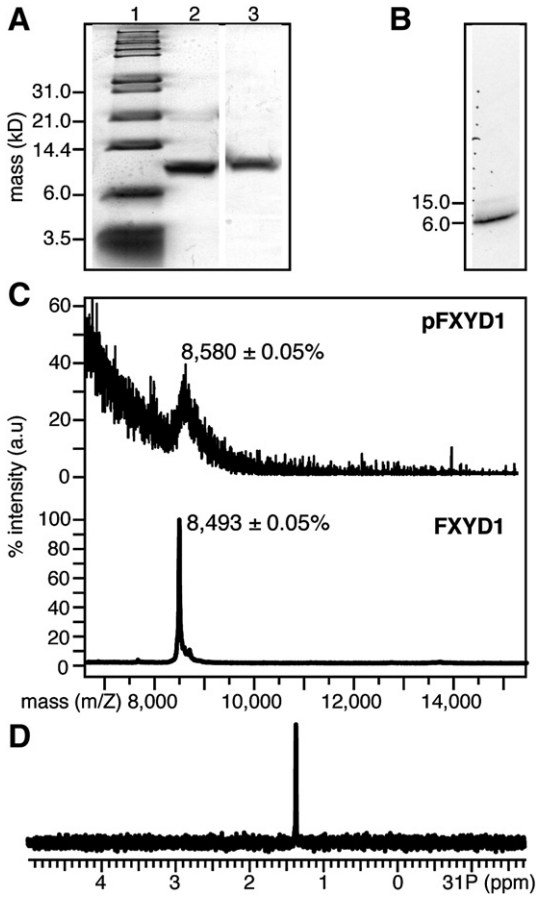

Fig. 2. PKA phosphorylates FXYD1 at a single site and induces a mobility shift of the FXYD1 band on SDS-PAGE. (A) Coomassie stained SDS polyacrylamide gel showing bands for molecular weight standards (lane 1), FXYD1 (lane 2), and pFXYD1 (lane 3). (B) Visualization of ^{32}P-labeled pFXYD1 by radio imaging. (C) MALDI-TOF spectra of pFXYD1 and FXYD1. (D) ^{31}P NMR of pFXYD1 in micelles.

2.3. Computational methods

Calculations to generate a molecular model of the α/β/FXYD1 Na,K-ATPase complex were performed using XPLOR-NIH [38]. The model was generated using the NMR structure of FXYD1 (PDB: 2JO1) [27], which includes all 72 residues of FXYD1, and the crystal structure of the pig kidney Na,K-ATPase (PDB: 3B8E) [25], which consists of residues 19–1016 of the 1016-residue α1 subunit, transmembrane residues 28–73 of the 303-residue β1 subunit, and transmembrane residues 23–51 of the 66-residue FXYD2a subunit. Missing hydrogens were added using XPLOR-NIH.

First, the coordinates of FXYD2 in the crystal structure were replaced with those of FXYD1 by aligning the CA atoms of their homologous transmembrane helices (FXYD1 residues Gly19-Gly31, FXYD2 residues G29–G41). The average RMSD between the transmembrane CA atoms of the two aligned segments was 1.19 Å.

Second, the resulting coordinates for the α/β/FXYD1 complex were subjected to 4 stages of Cartesian coordinate Powell minimization, where energy terms for covalent and non bonded interactions were introduced gradually as follows: 100 steps with a term for covalent bonds ($k = 1$); 500 steps with terms for covalent bonds and bond angles; 500 steps with terms for covalent bonds, bond angles and improper dihedral angles; and 500 steps with terms for covalent bonds, bond angles, improper dihedral angles, and weak non-bonded van der Waals interactions ($k_{VDW} = 0.01$ kcal mol^{-1} Å^{-4}; $k_{rad} = 0.8$).

Third, this minimized starting structure was subjected to a high-temperature semi-rigid body simulated annealing [39], using internal coordinates dynamics [40], to optimize the interface between FXYD1 and the α subunit. In this step, all the α, β, and FXYD1 atoms were held fixed, except those of the side chains (from CG onward) of FXYD1 and of the αM9 transmembrane helix (Lys945–Tyr963). These side chains were allowed both rotational and translational degrees of freedom. The energy function included terms for covalent geometry, Van der Waals contacts, and the torsion angle database Rama potential [41], to select preferred side chain conformations relative to the backbone dihedral angles. The energy terms were ramped as: $k_{ang} = 0.4$–1.0 kcal mol^{-1} deg^{-2}; $k_{imp} = 0.1$–1.0 kcal mol^{-1} deg^{-2}; $k_{RAMA} = 0.02$–0.2; $k_{VDW} = 0.002$–4.0 kcal mol^{-1} Å^{-4}; $k_{rad} = 0.4$–0.8. The final model consists of nearly the entire α subunit (998 out of

1016 residues), the transmembrane domain of the β subunit (46 out of 303 residues), and the entire FXYD1 subunit (72 residues). Compared to the coordinates of the original NMR and crystal structures deposited in the PDB, the final coordinates for α, β, and FXYD1 have respective average pairwise RMSDs of 0.27 Å, 0.32 Å, and 0.17 Å for the backbone atoms, and of 0.49 Å, 0.46 Å, and 1.74 Å for non-hydrogen atoms.

Molecular structures were visualized with the program Pymol [42]. Electrostatic potentials were calculated in units of kT/e, where *k* is the Boltzmann constant, T is the absolute temperature, and e is the proton charge, using the program PDB2PQR [43]. Electrostatic potentials were projected on the solvent accessible surfaces using the program APBS [44]. XPLOR and PDB2PQR calculations with pFXYD1 were performed after replacing Ser68 with mono-protonated phosphoserine, as expected at pH 5.

3. Results and discussion

3.1. Phosphorylation of FXYD1 by PKA

In vitro phosphorylation by PKA caused FXYD1 to migrate at a slightly higher apparent molecular weight on SDS-PAGE (Fig. 2A). This effect is likely due to the 80 Da mass increase from the addition of HPO_3, combined with the negative charge of the phosphate group causing less SDS to bind the protein. The absence of a band at lower molecular weight indicates that large-scale phosphorylation of FXYD1 is obtained with nearly 100% efficiency, since the size exclusion chromatography step used to isolate pFXYD1 from the enzymatic reaction mixture would not be able to separate the phosphorylated and non-phosphorylated proteins. Phosphorylation was also assessed by ^{32}P radio imaging (Fig. 2B) and by mass spectrometry, which shows the characteristic 80 Da mass increase within the ±0.05% range of the experimental error (Fig. 2C). In the NMR sample, single site phosphorylation was further confirmed by the ^{31}P NMR spectrum of pFXYD1 in micelles (Fig. 2D), which displays a single peak at the expected chemical shift frequency for phosphoserine at pH 5 [45,46].

3.2. Effects of Ser68 phosphorylation on FXYD1 conformation

To examine the effects of PKA phosphorylation we first compared the $^{1}H/^{15}N$ HSQC NMR spectra of FXYD1, pFXYD1 and the mutant FXYD1(S68D). ^{1}H and ^{15}N chemical shifts from protein backbone amide groups are very sensitive to changes in chemical environment and in protein conformation and, in other proteins, phosphorylation has been shown to induce chemical shift changes as large as several ppm due to electrostatic effects or to minor local conformational changes in the vicinity of the negatively charged phosphate group [47–52].

The HSQC spectra of FXYD1, pFXYD1 and FXYD1(S68D) all exhibit excellent frequency dispersion and a single peak for each amide site (Fig. 3), indicating that both pFXYD1 and FXYD1(S68D) adopt uniquely folded conformations. Furthermore, the spectrum of pFXYD1 shows no evidence of peaks from non-phosphorylated protein, confirming the presence of a single (>90%) phosphorylated species in the sample. Both the spectra of pFXYD1 and FXYD1(S68D) exhibit extensive overlap with the spectrum of FXYD1, indicating that the protein does not undergo a major conformational change upon either Ser68 phosphorylation or mutation to Asp. Peaks from residues 1–54, which include the transmembrane domain, are not perturbed at all and could be assigned to specific amino acids by direct comparison with the previously assigned spectrum of FXYD1 [27]. However, peaks from the cytoplasmic helix (h4), which contains the phosphorylation site, exhibited significant changes in both ^{1}H and ^{15}N chemical shifts. These peaks could not be assigned by direct comparison and required the use of $^{1}H/^{15}N$ NOESY-HSQC experiments.

Maps of the chemical shift changes resulting from phosphorylation or Asp mutation in the NMR spectra of pFXYD1 and FXYD1(S68D) show that the perturbation at Ser68 is detected throughout the length of helix h4 (Fig. 4). To determine whether the NMR frequency changes reflect a conformational change in this region or the electrostatics effects of the negatively charged phosphate group, we examined several key NMR indicators of structure (Fig. 5). The short range NOEs obtained from a three-dimensional $^{1}H/^{15}N$ NOESY-HSQC spectrum for

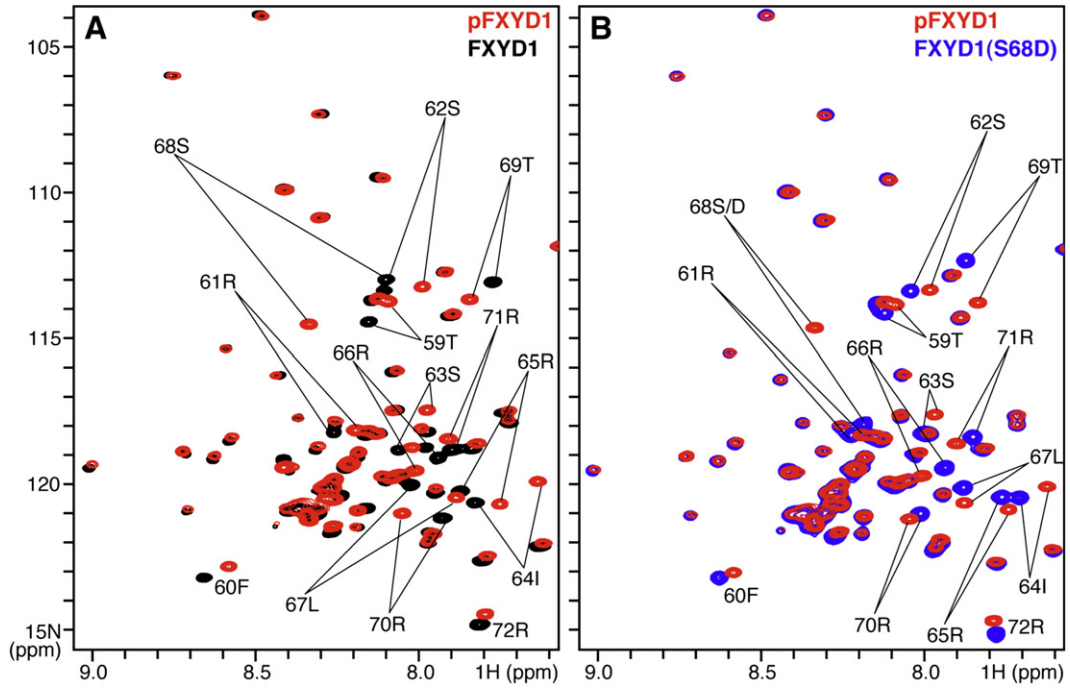

Fig. 3. NMR $^{1}H/^{15}N$ HSQC spectra of uniformly ^{15}N-labeled FXYD1 (black), pFXYD1 (red) and FXYD1(S68D) (blue). Residues 59 to 72 including helix h4 are indicated. (A) Overlapped spectra of FXYD1 and pFXYD1. (B) Overlapped spectra of pFXYD1 and FXYD1(S68D).

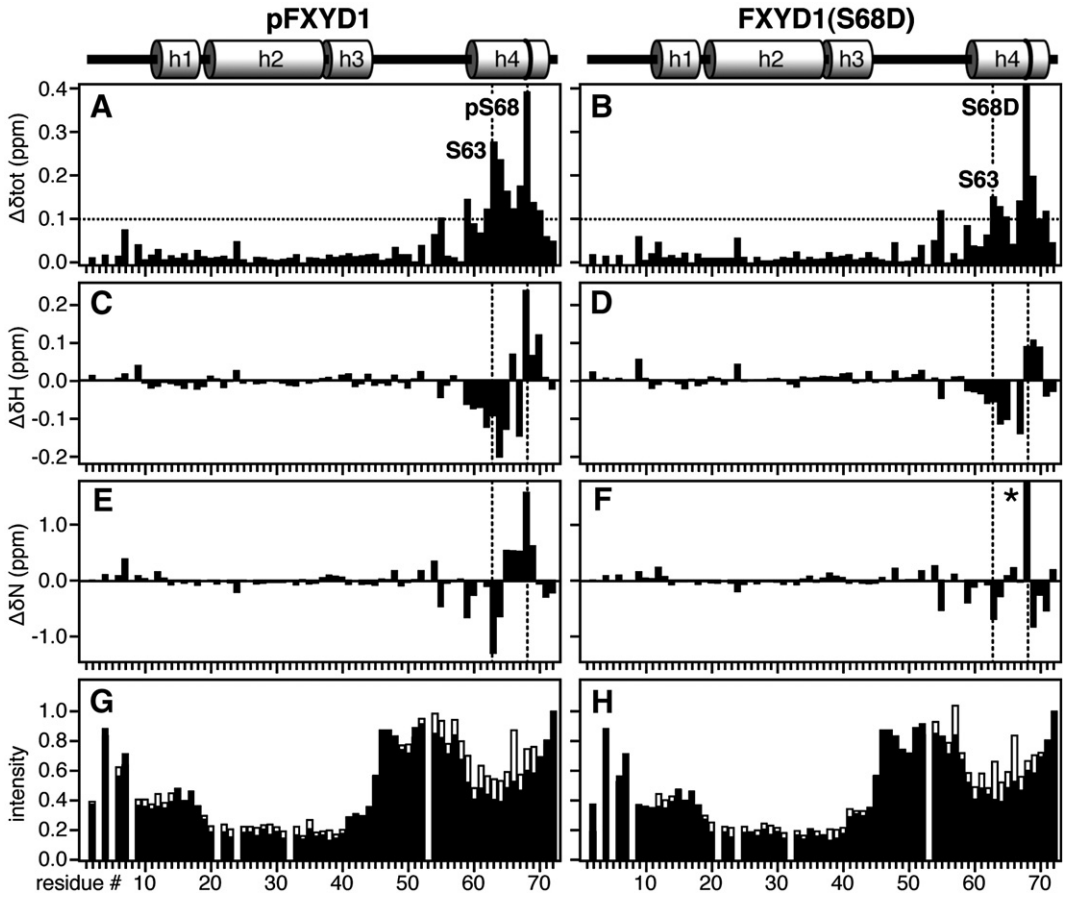

Fig. 4. Effects of S68 phosphorylation or S68D mutation on $^{1}H/^{15}N$ HSQC chemical shifts and peak intensities. The helical regions determined in the structure of FXYD1 are shown at the top. (A, B) Combined change in ^{1}H and ^{15}N chemical shifts ($\Delta\delta tot = [(\Delta\delta H)^2 + (\Delta\delta N/5)^2]^{1/2}$). $\Delta\delta N$ is scaled by 1/5 to account for the 5-fold difference between the chemical shift dispersions of ^{15}N and ^{1}H. The S68D peak has $\Delta\delta tot = 0.97$ ppm. (C, D) Changes in ^{1}H chemical shift for pFXYD1 ($\Delta\delta H = \delta H_{pFXYD1} - \delta H_{FXYD1}$) or FXYD1(S68D) ($\Delta\delta H = \delta H_{FXYD1(S68D)} - \delta H_{FXYD1}$). (E, F) Changes in ^{15}N chemical shift for pFXYD1 ($\Delta\delta N = \delta N_{pFXYD1} - \delta N_{FXYD1}$) or FXYD1(S68D) ($\Delta\delta N = \delta N_{FXYD1(S68D)} - \delta N_{FXYD1}$). Residue S68D (*) has $\Delta\delta N = 4.84$ ppm. (G, H) Normalized peak intensities for FXYD1 (black) and pFXYD1 or FXYD1(S68D) (white). Positions that are left blank correspond to Pro or overlapped resonances.

amide sites that are less than 4 residues apart have a similar pattern in both FXYD1 and pFXYD1, indicating the absence of conformational change in h4 after phosphorylation (Fig. 5A). Furthermore, a comparative TALOS analysis of the chemical shifts measured for pFXYD1 and FXYD1 indicates that residues 60 to 70 retain an α-helical conformation after Ser68 phosphorylation (Fig. 5B). Although this analysis was limited to HN and HA chemical shifts, all of the helical regions, including h4, that were previously determined in the structure of FXYD1, using the complete set of ^{13}C, ^{15}N, and ^{1}H chemical shifts plus RDCs and NOEs [6,27], were correctly identified in both FXYD1 and pFXYD1.

The paramagnetic electrons in the Mn^{2+} ion induce distance-dependent broadening of peaks from protein sites that are solvent-exposed, without affecting those from sites in the hydrophobic interior of the micelle. The addition of $MnCl_2$ to FXYD1(S68D) resulted in substantial line broadening and disappearance of peaks from residues in the N- and C-terminal regions and in the flexible linker, while peaks from the transmembrane region and from helix h4 retained significant or full intensity, indicative of strong association with the hydrophobic micelle. This is similar to our previous observations for FXYD1 in micelles [27] and to previous observations for FXYD1 in lipid bilayers [53,54]. The data indicate that the basic L-shaped arrangement of the protein, with one transmembrane segment and helix h4 embedded parallel to the micelle/membrane surface, is not significantly perturbed by the presence of a negative charge at residue 68. Thus, since the protein conformation is not significantly altered, we conclude that the observed frequency changes in the spectra of pFXYD1 and FXYD1(S68D) must be due to the introduction of a negative charge at residue 68.

The significant downfield shifts (to higher frequency) observed for the amide resonance of Ser68 after phosphorylation ($\Delta\delta H = 0.24$ ppm; $\Delta\delta N = 1.57$ ppm), or after mutation to Asp ($\Delta\delta H = 0.09$ ppm; $\Delta\delta N = 4.84$ ppm), reflect a deshielding of the corresponding amide site from the external magnetic field (Fig. 4C–F). The inductive electron-withdrawing effect of the negatively charged phosphate may be expected to influence the amide hydrogen bonds of residue Ser68, as well as those of Thr69 and Arg70. Indeed, the ^{1}H frequencies of these residues are all shifted downfield compared to their positions in the spectrum of FXYD1 and a similar effect is observed for the ^{1}H frequencies of Thr69 and Arg70 in the spectrum of FXYD1(S68D). The frequency changes extend along the length of helix h4, and decrease in magnitude with increasing spatial distance from residue 68. Interestingly, the frequency changes follow a general trend with peaks from amides on the C-terminal side of Ser68 moving downfield, and peaks from amides N-terminal to Ser68 moving upfield (to lower frequency). This polarized peak perturbation pattern may reflect the interactions of the negatively charged phosphate or Asp with the macrodipole of helix h4, affecting the electronic environment throughout the helix, as previously suggested for the Ser-phosphorylated form of His-containing protein [49].

It is also interesting to note that both Ser68 phosphorylation and Asp mutation induce very significant upfield frequency changes for the peak of Ser63, a residue that is phosphorylated by PKC. Although the significance of this effect cannot be determined from the present

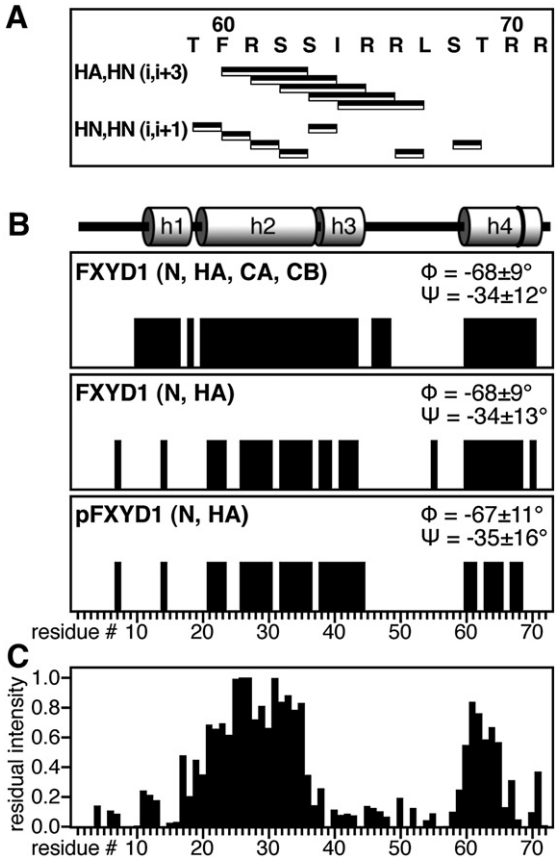

Fig. 5. Effects of S68 phosphorylation or S68D mutation on the conformation of FXYD1. (A) Sequential and medium range H-H NOEs measured for FXYD1 (black) and pFXYD1 (white). (B) TALOS analysis using N, HA, CA, and CB chemical shifts of FXYD1 (top), only N and HA chemical shifts of FXYD1 (middle), or only N and HA chemical shifts of pFXYD1 (bottom). For each residue only "good" TALOS results with 9 or more matches to the database having dihedral angles in a consistent region of the Ramachandran plot are shown (see Materials and methods). The average backbone dihedral angles, obtained for residues 60–70 in helix h4, are reported in each panel. The helical regions determined in the structure of FXYD1 are shown at the top. (C) Residual peak intensity (Ires) measured for FXYD1(S68D) after addition of 1.8 mM $MnCl_2$ ($Ires = I_{+Mn}/I_{-Mn}$).

data, this may point to a synergistic relationship between PKA and PKC phosphorylation, where PKA phosphorylation at Ser68 primes helix h4 for subsequent PKC phosphorylation at other sites. This could be important for regulating the transport of FXYD1 from the ER to the plasma membrane, as proposed for the NMDA NR1 subunit [12].

Previously, we have used $^{1}H/^{15}N$ HSQC peak intensities and heteronuclear $^{1}H–^{15}N$ NOEs to characterize the backbone dynamics of FXYD1 in micelles [6,27]. Resonance intensities correlate with resonance line widths, which are excellent indicators of local backbone dynamics and can be easily measured as peak heights in the HSQC spectra of proteins. Large-amplitude backbone motions that are rapid compared to the overall reorientation rate of the protein reduce the line widths and increase the peak intensities, while lower intensities are observed for less mobile regions or sites undergoing chemical exchange in the intermediate range of the μs–ms time scale.

For FXYD1, helices h2 and h3 in the transmembrane region are rigidly connected and have peaks with similar intensities that plateau at a minimum value in the membrane interior. In contrast, h1 and h4 are somewhat more dynamic, while residues in the termini and in the linker between h3 and h4 have peaks with much greater intensities, reflecting much greater local dynamics (Figs. 4G and H, black). PKA phosphorylation and Ser68Asp mutation both produce a very modest increase in intensity for peaks from h4 (Fig. 4G and H, white), consistent with a modest increase in backbone dynamics in this region of the protein. A change in the orientation of h4 relative to the diffusion tensor of the protein/micelle assembly could produce line narrowing effects similar to those observed for pFXYD1 and FXYD1 (S68D). However, the observation of significant protection from Mn^{2+}-induced paramagnetic broadening in h4 indicates that a major change in the helix orientation away from the micelle/membrane surface is not the cause of line narrowing in the spectra of pFXYD1 and FXYD1(S68D).

Our previous NMR studies of FXYD1 indicated that helix h4 could undergo rotational excursions as large as 40° around its long axis (Fig. 6A), while maintaining the helix amphiphilic polarity relative to the micelle surface, with apolar residues facing the micelle lipophilic interior and polar residues facing the aqueous environment [27]. The peak intensity profiles suggest that this is not dramatically changed by PKA phosphorylation. However, a slight increase in dynamics after phosphorylation could reflect a slightly increased rate of excursions of helix h4 away from the micelle/membrane surface into the cytoplasm (Fig. 6B), or a slightly increased rate of helix reorientation in the plane of the membrane surface (Fig. 6C). For phospholamban, the analogous but unrelated regulator of the sarcoplasmic reticulum Ca-ATPase, phosphorylation at Ser16 and its phosphorylation mimicking mutation to Glu also induce a modest change in protein backbone dynamics near residue 16 [50,55].

3.3. Implications for the interactions of FXYD1 with the Na,K-ATPase

Taken together, the absence of chemical shift or peak intensity changes outside helix h4, the polarized pattern of chemical shift perturbations along the helix length, and the modest increase in h4 backbone dynamics, all indicate that PKA phosphorylation does not induce major changes in either the backbone conformation or

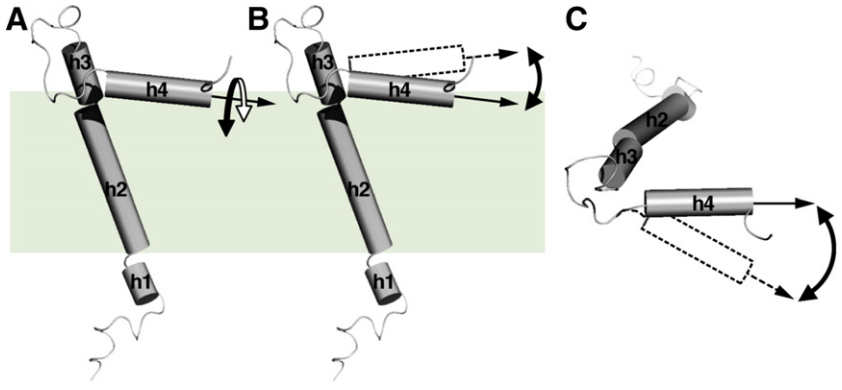

Fig. 6. Three types of helix h4 reorientation that could give rise to increased rate of dynamics while maintaining the membrane surface association of helix h4. (A) Reorientation around the helix long axis. (B) Rotational excursions away from the membrane surface. (C) Reorientation in the plane of the membrane surface viewed from the cytoplasm.

dynamics of FXYD1. Neither the helical structure nor the location of h4 at the micelle–water interface appears to be significantly perturbed by phosphorylation. A predisposition for membrane surface association is indicated by the amphiphilic character of h4 and demonstrated by the NMR structure of FXYD1 in micelles [27] as well as by solid-state NMR data in lipid bilayers [53,54]. The $MnCl_2$ broadening profile observed for FXYD1(S68D) (Fig. 5C) indicates that this arrangement is unchanged by phosphorylation. It is possible that helix h4 adopts a different orientation in the presence of the Na,K-ATPase α subunit from that observed for isolated FXYD1. However, the lack of electron density for the cytoplasmic domains of FXYD2 in the crystal structure of pig kidney Na,K-ATPase, and of FXYD10 in the structure of the shark rectal gland Na,K-ATPase, indicates the absence of a strong structural interaction between the FXYD cytoplasmic domains and α.

A major phosphorylation-induced conformational change of FXYD1 was proposed in a recent study measuring fluorescence energy transfer between two fluorescent proteins, one linked to the C-terminus of FXYD1 and the other to the N-terminus of α1 [56]. These experiments are complicated by the very large sizes of the fluorescent proteins (~30 kDa) compared to the size of FXYD1 (~8 kDa), and also by the dependence of the Na,K-ATPase and FXYD1 plasma membrane expression levels on PKA and PKC phosphorylation [9,14]. However, phosphorylation at more than one of the three sites (Ser63, Ser69, Thr69) could be required to trigger a conformational change in FXYD1. Furthermore, a conformational change involving reorientation of helix h4 in the plane of the micelle/membrane surface (i.e. around an axis perpendicular to the membrane plane, as shown in Figs. 6C or 8B) would maintain its amphiphilic polarity at the membrane surface, and cannot be excluded based on the NMR data reported in this study.

The NMR data together with a comparison of the calculated surface electrostatic potentials for FXYD1 and pFXYD1 indicate that the effects of PKA phosphorylation could be due to the presence of the negative charged phosphate group at the membrane surface, which could influence the interactions of residues in h4 with each other, with α, and with the membrane phospholipid headgroups. Electrostatic repulsions between the negatively charged phosphate and the negatively charged micelle/membrane surface, together with potential changes in the hydrogen bonding pattern, may be sufficient to account for a slight increase in conformational dynamics of h4. Since the Na,K-ATPase is sensitive to membrane potential [57,58], these combined changes in electrostatics at the membrane surface could also account for the opposing effects of FXYD1 and pFXYD1 on the functional properties of the pump.

3.4. Structural model of the α/β/FXYD1 complex

As an initial step toward understanding the association of FXYD1 with the Na,K-ATPase, we generated a model of the α/β/FXYD1 complex by replacing the coordinates of endogenous FXYD2 in the crystal structure of the pump from pig kidney [25] with those of FXYD1 determined by NMR [27], and performing molecular dynamics to optimize the α/FXYD1 interface (Figs. 7, 8A). The crystal structures indicate an intimate association between the FXYD and αM9 transmembrane helices, mediated by two glycines that are fully conserved in all FXYD proteins (FXYD1 Gly20 and Gly31). Because only the side chains of FXYD1 and αM9 were allowed rotational and translational degrees of freedom during the calculation, the backbone conformations of the α, β and FXYD1 subunits in the resulting model are unchanged from those of the starting coordinates, and the orientation of helix h4 on the membrane surface is the same as that originally determined by the combination of solid-state NMR in lipid bilayers and solution NMR in micelles [27,54]. Notably, the resulting model indicates that the membrane surface orientation of helix h4 is compatible with the FXYD1/αM9 transmembrane association mediated by Gly20 and Gly31. It is also interesting to note that the orientation of FXYD1 in the model is the same as the orientation that was determined for isolated FXYD1 in lipid bilayer membranes [27,54]. This suggests that the structure of isolated FXYD1 is representative of the Na,K-ATPase-bound structure and that, aside from the Gly-mediated association with αM9, there could be other FXYD-specific factors (e.g. electrostatics) that predispose FXYD1 to adopt a specific orientation within the membrane.

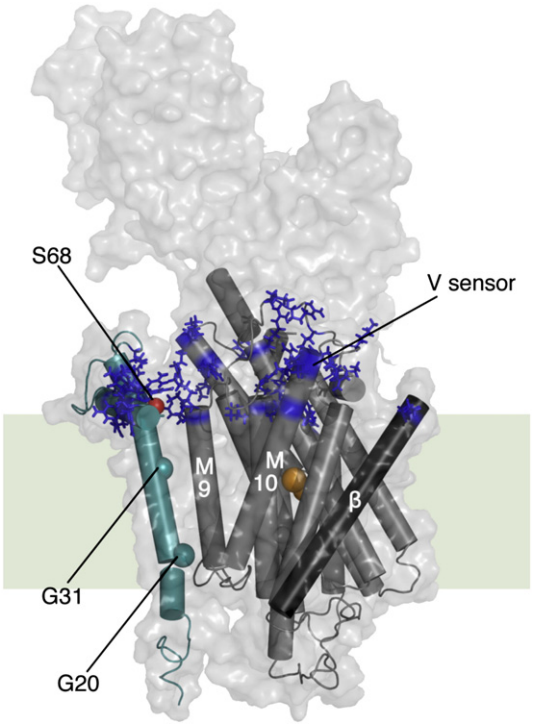

Fig. 7. Structural model of the α/β/FXYD1 Na,K-ATPase complex. FXYD1 (teal), and α β (gray) transmembrane helices are shown within the solvent-accessible surface of the complex. Arg and Lys side chains at the cytoplasmic membrane surface are blue. Occluded Rb^+/K^+ ions identified in the crystal structure of kidney Na,K-ATPase are yellow. The proposed voltage-sensing module is at the end of αM10. CA atoms of FXYD1 Gly20 and Gly31 and FXYD1 Ser68 phosphate (red) are shown as spheres. The gray slab represents the membrane thickness.

The crystal structure of pig kidney Na,K-ATPase highlighted a highly electropositive region near the cytoplasmic membrane surface and the Na^+/K^+ ion binding sites of the α subunit. This region is composed of Arg and Lys residues located at the cytoplasmic ends of the α transmembrane helices and in their cytoplasmic connecting loops, and includes Arg1003, Arg1004 and Arg1005 at the end of αM10, which were proposed to constitute a voltage-sensing module [25] analogous to the voltage sensors of potassium channels [59,60]. In the α/β/FXYD1 model the membrane surface location of FXYD1 h4 further contributes to this network of positive charges, suggesting that FXYD1 could influence Na,K-ATPase ion transport by regulating the membrane electrostatic potential near the ion binding sites (Figs. 7, 8A). The introduction of negative charge by phosphorylation would alter the surface electrostatics in h4 and this could have profound effects on ion binding and transport by the α subunit.

In FXYD1 and in other FXYD proteins the short helical extension (h3) of the transmembrane helix (h2) could also contribute to this effect, due to its highly basic nature and membrane-surface location. In all the FXYD proteins h3 is encoded by a single exon [6] and its amino acid sequence varies in its use of Arg and Lys residues. Although both are positively charged, these residues differ in their ability to form hydrogen bonds (Arg>Lys) and in their charge delocalization (Arg>Lys). Thus, their discrete use among the FXYD family members could provide a further means of modulating their activities.

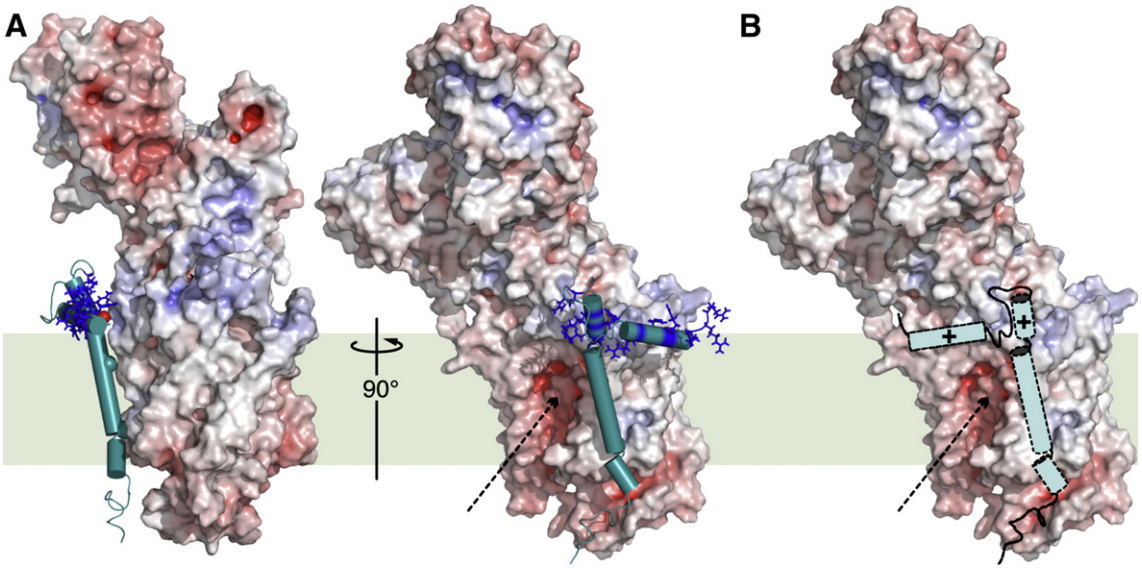

Fig. 8. Structural model of the α/β/FXYD1 complex and potential alternative orientation of FXYD1 helix h4. (A) 90° views showing the backbone of FXYD1 (teal), and the solvent accessible surface of α/β colored by electrostatic potential, with blue to red color gradation spanning a range of ± 15 kT/e from positive to negative potential. FXYD1 helix h4 is in the conformation determined in the NMR structure and the FXYD1/αM9 interfaced was optimized by molecular dynamics. Arg and Lys side chains in h3 and h4 are in blue. (B) Alternative conformation of FXYD1 where h4 associates with both the membrane surface and the negatively charged crevice (dashed arrow) leading to the ion binding pocket in center of α.

Recent simulations by Jogini and Roux [60] indicate that specific Arg side chains in the KvAP channel voltage sensor are paired with one or more lipid phosphodiester groups at the membrane-water interface, dramatically influencing the local electric field. This is consistent with recent findings of a negatively charged lipid phosphodiester requirement for channel function [61] and provides an attractive explanation for the voltage sensor mechanism. Similar requirements for negatively charged phospholipids have been reported for optimal Na,K-ATPase activity (see [22,62] and references therein), and Arg residues in FXYD1 h3 and h4 could interact with the lipid headgroups at the membrane-water interface, to modulate the membrane electrostatics near the Na/K-ATPase ion binding sites. Furthermore, in the KvAP simulation small vertical motions of the Arg guanidinium groups along the direction of the membrane normal are predicted to produce large transmembrane charge fluctuations. Similarly, the slightly increased dynamics observed for Ser68 phosphorylation, combined with the addition of a negatively charged phosphate group, could produce transmembrane charge fluctuations with profound consequences for Na,K-ATPase ion transport.

Phosphorylation of the Ca-ATPase regulator phospholamban also induces a small increase in backbone dynamics [50,55]. This is accompanied by a partial unwinding [50] or loosening [51] of the cytoplasmic helix in the monomeric form of the protein, while the pentameric form is reported to exhibit little evidence of conformational change [55] and to conserve the α-helical structure around the Ser16 phosphorylation site [63]. Furthermore, Ser16 phosphorylation does not appear to affect the membrane surface association of the isolated cytoplasmic domain of phospholamban [53]. Interestingly, the Ser16 phosphorylation site of phospholamban is in a short linker between the transmembrane and cytoplasmic helices, and situated near the membrane surface just like Ser68 in FXYD1. Thus, the modulation of membrane surface potential may be a common mechanism for the regulation of P-type ATPases by their accessory proteins.

Finally we note that alternative orientations of h4 that maintain the helix amphiphilic polarity and its membrane surface association can be envisioned including one that would place helix h4 near a negatively charged crevice formed by transmembrane helices αM2, αM4, and αM6, leading to the ion binding pocket in center of the α subunit (e.g. Fig. 8B). Acidic residues in this region of α are conserved to allow the approach of cations but exclude anions through the pump, and reversing the charge at just one of those positions converts the Na,K-ATPase channel from cation selective to anion selective [64]. The net positive charge of helix h4 and its modulation by phosphorylation could have a major influence on the electrostatics around the α anionic crevice, with potentially important consequences for ion binding. Three-dimensional structure determination of the FXYD1/Na,K-ATPase complex is essential for understanding the function of FXYD1 and the role of FXYD1 phosphorylation. The α/β/FXYD1 structural model and the data presented in this study provide some initial insights.

Acknowledgements

We thank Yong Huang and Nathan Baker for their assistance with PDB2PQR and APBS, and Scott Williams and Tomas Mustelin for their assistance with ^{32}P-labeled ATP experiments. This research was supported by the National Institutes of Health. It utilized the Burnham Institute NMR Facility, supported by a grant from the National Institutes of Health (CA030199).

References

[1] F. Cornelius, Y.A. Mahmmoud, Functional modulation of the sodium pump: the regulatory proteins "Fixit", News Physiol. Sci. 18 (2003) 119–124.
[2] H. Garty, S.J. Karlish, Role of fxyd proteins in ion transport, Annu. Rev. Physiol. 68 (2006) 431–459.
[3] K. Geering, FXYD proteins: new regulators of Na-K-ATPase, Am. J. Physiol. Renal. Physiol. 290 (2006) F241–F250.
[4] G. Blanco, R.W. Mercer, Isozymes of the Na-K-ATPase: heterogeneity in structure, diversity in function, Am. J. Physiol. 275 (1998) F633–F650.
[5] K.J. Sweadner, E. Rael, The FXYD gene family of small ion transport regulators or channels: cDNA sequence, protein signature sequence, and expression, Genomics 68 (2000) 41–56.
[6] C.M. Franzin, J. Yu, K. Thai, J. Choi, F.M. Marassi, Correlation of gene and protein structures in the FXYD family proteins, J. Mol. Biol. 354 (2005) 743–750.
[7] C.J. Palmer, B.T. Scott, L.R. Jones, Purification and complete sequence determination of the major plasma membrane substrate for cAMP-dependent protein kinase and protein kinase C in myocardium, J. Biol. Chem. 266 (1991) 11126–11130.
[8] S.I. Walaas, A.J. Czernik, O.K. Olstad, K. Sletten, O. Walaas, Protein kinase C and cyclic AMP-dependent protein kinase phosphorylate phospholemman, an insulin and adrenaline-regulated membrane phosphoprotein, at specific sites in the carboxy terminal domain, Biochem. J. 304 (1994) 635–640.
[9] K.L. Lansbery, L.C. Burcea, M.L. Mendenhall, R.W. Mercer, Cytoplasmic targeting signals mediate delivery of phospholemman to the plasma membrane, Am. J. Physiol. Cell Physiol. 290 (2006) C1275–C1286.

[10] S. Bibert, S. Roy, D. Schaer, J.D. Horisberger, K. Geering, Phosphorylation of phospholemman (FXYD1) by protein kinases A and C modulates distinct Na,K-ATPase isozymes, J. Biol. Chem. 283 (2008) 476–486.
[11] K. Michelsen, H. Yuan, B. Schwappach, Hide and run. Arginine-based endoplasmic-reticulum-sorting motifs in the assembly of heteromultimeric membrane proteins, EMBO Rep. 6 (2005) 717–722.
[12] D.B. Scott, T.A. Blanpied, M.D. Ehlers, Coordinated PKA and PKC phosphorylation suppresses RXR-mediated ER retention and regulates the surface delivery of NMDA receptors, Neuropharmacology 45 (2003) 755–767.
[13] J.P. Mounsey, K.P. Lu, M.K. Patel, Z.H. Chen, L.T. Horne, J.E. John 3rd, A.R. Means, L.R. Jones, J.R. Moorman, Modulation of Xenopus oocyte-expressed phospholemman-induced ion currents by co-expression of protein kinases, Biochim. Biophys. Acta 1451 (1999) 305–318.
[14] B. Kristensen, S. Birkelund, P.L. Jorgensen, Trafficking of Na,K-ATPase fused to enhanced green fluorescent protein is mediated by protein kinase A or C, J. Membr. Biol. 191 (2003) 25–36.
[15] S. Despa, J. Bossuyt, F. Han, K.S. Ginsburg, L.G. Jia, H. Kutchai, A.L. Tucker, D.M. Bers, Phospholemman-phosphorylation mediates the beta-adrenergic effects on Na/K pump function in cardiac myocytes, Circ. Res. 97 (2005) 252–259.
[16] B.Z. Silverman, W. Fuller, P. Eaton, J. Deng, J.R. Moorman, J.Y. Cheung, A.F. James, M.J. Shattock, Serine 68 phosphorylation of phospholemman: acute isoform-specific activation of cardiac Na/K ATPase, Cardiovasc. Res. 65 (2005) 93–103.
[17] F. Han, J. Bossuyt, S. Despa, A.L. Tucker, D.M. Bers, Phospholemman phosphorylation mediates the protein kinase C-dependent effects on Na+/K+ pump function in cardiac myocytes, Circ. Res. 99 (2006) 1376–1383.
[18] D. Pavlovic, W. Fuller, M.J. Shattock, The intracellular region of FXYD1 is sufficient to regulate cardiac Na/K ATPase, FASEB J. (2007).
[19] W. Fuller, J. Howie, L. McLatchie, R. Weber, C.J. Hastie, K. Burness, D. Pavlovic, M.J. Shattock, Fxyd1 phosphorylation *in vitro* and in adult rat cardiac myocytes: threonine 69 is a novel substrate for protein kinase C, Am. J. Physiol. Cell Physiol. (2009).
[20] G. Crambert, M. Fuzesi, H. Garty, S. Karlish, K. Geering, Phospholemman (FXYD1) associates with Na,K-ATPase and regulates its transport properties, Proc. Natl. Acad. Sci. U. S. A. 99 (2002) 11476–11481.
[21] Y. Lifshitz, M. Lindzen, H. Garty, S.J. Karlish, Functional interactions of phospholemman (PLM) (FXYD1) with Na+,K+-ATPase. Purification of alpha1/beta1/PLM complexes expressed in *Pichia pastoris*, J. Biol. Chem. 281 (2006) 15790–15799.
[22] Y. Lifshitz, E. Petrovich, H. Haviv, R. Goldshleger, D.M. Tal, H. Garty, S.J. Karlish, Purification of the human alpha2 Isoform of Na,K-ATPase expressed in Pichia pastoris. Stabilization by lipids and FXYD1, Biochemistry 46 (2007) 14937–14950.
[23] J.R. Bell, E. Kennington, W. Fuller, K. Dighe, P. Donoghue, J.E. Clark, L.G. Jia, A.L. Tucker, J.R. Moorman, M.S. Marber, P. Eaton, M.J. Dunn, M.J. Shattock, Characterization of the phospholemman knockout mouse heart: depressed left ventricular function with increased Na-K-ATPase activity, Am. J. Physiol. Heart Circ. Physiol. 294 (2008) H613–H621.
[24] X.Q. Zhang, J.R. Moorman, B.A. Ahlers, L.L. Carl, D.E. Lake, J. Song, J.P. Mounsey, A.L. Tucker, Y.M. Chan, L.I. Rothblum, R.C. Stahl, D.J. Carey, J.Y. Cheung, Phospholemman overexpression inhibits Na+-K+-ATPase in adult rat cardiac myocytes: relevance to decreased Na+ pump activity in postinfarction myocytes, J. Appl. Physiol. 100 (2006) 212–220.
[25] J.P. Morth, B.P. Pedersen, M.S. Toustrup-Jensen, T.L. Sorensen, J. Petersen, J.P. Andersen, B. Vilsen, P. Nissen, Crystal structure of the sodium-potassium pump, Nature 450 (2007) 1043–1049.
[26] T. Shinoda, H. Ogawa, F. Cornelius, C. Toyoshima, Crystal structure of the sodium-potassium pump at 2.4 A resolution, Nature 459 (2009) 446–450.
[27] P. Teriete, C.M. Franzin, J. Choi, F.M. Marassi, Structure of the Na,K-ATPase regulatory protein FXYD1 in micelles, Biochemistry 46 (2007) 6774–6783.
[28] C.M. Franzin, P. Teriete, F.M. Marassi, Structural similarity of a membrane protein in micelles and membranes, J. Am. Chem. Soc. 129 (2007) 8078–8079.
[29] K. Thai, J. Choi, C.M. Franzin, F.M. Marassi, Bcl-XL as a fusion protein for the high-level expression of membrane-associated proteins, Protein Sci. 14 (2005) 948–955.
[30] C.M. Rembold, M.L. Ripley, M.K. Meeks, L.M. Geddis, H.C. Kutchai, F.M. Marassi, J.Y. Cheung, J.R. Moorman, Serine 68 phospholemman phosphorylation during forskolin-induced swine carotid artery relaxation, J. Vasc. Res. 42 (2005) 483–491.
[31] H. Schagger, G. von Jagow, Tricine-sodium dodecyl sulfate-polyacrylamide gel electrophoresis for the separation of proteins in the range from 1 to 100 kDa, Anal. Biochem. 166 (1987) 368–379.
[32] S. Mori, C. Abeygunawardana, M.O. Johnson, P.C.M. Vanzijl, Improved sensitivity of HSQC spectra of exchanging protons at short interscan delays using a new fast HSQC (FHSQC) detection scheme that avoids water saturation, J. Magn. Reson. B 108 (1995) 94–98.
[33] A. Bax, S. Grzesiek, Methodological advances in protein NMR, Acc. Chem. Res. 26 (1993) 131–138.
[34] J. Cavanagh, W.J. Fairbrother, A.G. Palmer, N.J. Skelton, Protein NMR spectroscopy : principles and practice, Academic Press, San Diego, 1996.
[35] F. Delaglio, S. Grzesiek, G.W. Vuister, G. Zhu, J. Pfeifer, A. Bax, NMRPipe: a multidimensional spectral processing system based on UNIX pipes, J. Biomol. NMR 6 (1995) 277–293.
[36] T.D. Goddard, D.G. Kneller, SPARKY 3, University of California, San Francisco, 2004.
[37] G. Cornilescu, F. Delaglio, A. Bax, Protein backbone angle restraints from searching a database for chemical shift and sequence homology, J. Biomol. NMR 13 (1999) 289–302.
[38] C.D. Schwieters, J.J. Kuszewski, N. Tjandra, G. Marius Clore, The Xplor-NIH NMR molecular structure determination package, J. Magn. Reson. 160 (2003) 65–73.
[39] G.M. Clore, Accurate and rapid docking of protein-protein complexes on the basis of intermolecular nuclear overhauser enhancement data and dipolar couplings by rigid body minimization, Proc. Natl. Acad. Sci. U. S. A. 97 (2000) 9021–9025.
[40] C.D. Schwieters, G.M. Clore, Internal coordinates for molecular dynamics and minimization in structure determination and refinement, J. Magn. Reson. 152 (2001) 288–302.
[41] J. Kuszewski, A.M. Gronenborn, G.M. Clore, Improvements and extensions in the conformational database potential for the refinement of NMR and X-ray structures of proteins and nucleic acids, J. Magn. Reson. 125 (1997) 171–177.
[42] W.L. DeLano, PyMol, www.pymol.org (2005).
[43] T.J. Dolinsky, J.E. Nielsen, J.A. McCammon, N.A. Baker, PDB2PQR: an automated pipeline for the setup of Poisson–Boltzmann electrostatics calculations, Nucleic Acids Res. 32 (2004) W665–W667.
[44] N.A. Baker, D. Sept, S. Joseph, M.J. Holst, J.A. McCammon, Electrostatics of nanosystems: application to microtubules and the ribosome, Proc. Natl. Acad. Sci. U. S. A. 98 (2001) 10037–10041.
[45] H.J. Vogel, W.A. Bridger, Phosphorus-31 nuclear magnetic resonance studies of the two phosphoserine residues of hen egg white ovalbumin, Biochemistry 21 (1982) 5825–5831.
[46] S.P. Williams, W.A. Bridger, M.N. James, Characterization of the phosphoserine of pepsinogen using 31P nuclear magnetic resonance: corroboration of X-ray crystallographic results, Biochemistry 25 (1986) 6655–6659.
[47] P. Rajagopal, E.B. Waygood, R.E. Klevit, Structural consequences of histidine phosphorylation: NMR characterization of the phosphohistidine form of histidine-containing protein from *Bacillus subtilis* and *Escherichia coli*, Biochemistry 33 (1994) 15271–15282.
[48] S.M. Meyn, C. Seda, M. Campbell, K.L. Weiss, H. Hu, B. Pastrana-Rios, W.J. Chazin, The biochemical effect of Ser167 phosphorylation on *Chlamydomonas reinhardtii centrin*, Biochem. Biophys. Res. Commun. 342 (2006) 342–348.
[49] K. Pullen, P. Rajagopal, B.R. Branchini, M.E. Huffine, J. Reizer, M.H. Saier Jr., J.M. Scholtz, R.E. Klevit, Phosphorylation of serine-46 in HPr, a key regulatory protein in bacteria, results in stabilization of its solution structure, Protein Sci. 4 (1995) 2478–2486.
[50] E.E. Metcalfe, N.J. Traaseth, G. Veglia, Serine 16 phosphorylation induces an order-to-disorder transition in monomeric phospholamban, Biochemistry 44 (2005) 4386–4396.
[51] P. Pollesello, A. Annila, Structure of the 1-36 N-terminal fragment of human phospholamban phosphorylated at Ser-16 and Thr-17, Biophys. J. 83 (2002) 484–490.
[52] R.J. Mortishire-Smith, S.M. Pitzenberger, C.J. Burke, C.R. Middaugh, V.M. Garsky, R.G. Johnson, Solution structure of the cytoplasmic domain of phopholamban: phosphorylation leads to a local perturbation in secondary structure, Biochemistry 34 (1995) 7603–7613.
[53] J.C. Clayton, E. Hughes, D.A. Middleton, The cytoplasmic domains of phospholamban and phospholemman associate with phospholipid membrane surfaces, Biochemistry 44 (2005) 17016–17026.
[54] C.M. Franzin, X.M. Gong, K. Thai, J. Yu, F.M. Marassi, NMR of membrane proteins in micelles and bilayers: The FXYD family proteins, Methods 41 (2007) 398–408.
[55] K. Oxenoid, A.J. Rice, J.J. Chou, Comparing the structure and dynamics of phospholamban pentamer in its unphosphorylated and pseudo-phosphorylated states, Protein Sci. 16 (2007) 1977–1983.
[56] J. Bossuyt, S. Despa, J.L. Martin, D.M. Bers, Phospholemman phosphorylation alters its fluorescence resonance energy transfer with the Na/K-ATPase pump, J. Biol. Chem. 281 (2006) 32765–32773.
[57] H.J. Apell, S.J. Karlish, Functional properties of Na,K-ATPase, and their structural implications, as detected with biophysical techniques, J. Membr. Biol. 180 (2001) 1–9.
[58] D.C. Gadsby, R.F. Rakowski, P. De Weer, Extracellular access to the Na,K pump: pathway similar to ion channel, Science 260 (1993) 100–103.
[59] B. Roux, Lonely arginine seeks friendly environment, J. Gen. Physiol. 130 (2007) 233–236.
[60] V. Jogini, B. Roux, Dynamics of the Kv1.2 voltage-gated K+ channel in a membrane environment, Biophys. J. 93 (2007) 3070–3082.
[61] D. Schmidt, Q.X. Jiang, R. MacKinnon, Phospholipids and the origin of cationic gating charges in voltage sensors, Nature 444 (2006) 775–779.
[62] F. Cornelius, Y.A. Mahmmoud, Modulation of FXYD interaction with Na,K-ATPase by anionic phospholipids and protein kinase phosphorylation, Biochemistry (2007).
[63] S. Abu-Baker, G.A. Lorigan, Phospholamban and its phosphorylated form interact differently with lipid bilayers: a 31P, 2H, and 13C solid-state NMR spectroscopic study, Biochemistry 45 (2006) 13312–13322.
[64] N. Reyes, D.C. Gadsby, Ion permeation through the Na+,K+-ATPase, Nature 443 (2006) 470–474.